# WAVE INDUCED SURFACE CURRENTS ON THE GRAND BANKS

Charles Tang, William Perrie, Peter C. Smith
Bedford Institute of Oceanography
Ocean Sciences Division
Fisheries and Oceans Canada
Dartmouth, Nova Scotia, Canada

## 1. Introduction

Ocean surface waves have long been known to give rise to near-surface drift currents known as the Stokes drift. The amplitude of the Stokes drift is proportional to the square of the wave amplitude. Surface waves carry momentum equal to the water density multiplied by the vertically integrated Stokes drift. When waves dissipate, by means of viscous forces, turbulence, and/or wave breaking, this momentum is transferred to the mean *Eulerian* current (Jenkins, 1987).

In a study of the impact of waves on surface currents, Perrie et al. (2003) coupled the formulation of Jenkins (1989) to a simple linear diagnostic ocean model with an Ekman layer and a depth independent eddy viscosity to computer surface currents. They found that the wave effect could increase the surface currents by as much as 40%. In this paper, Jenkins' formulation is implemented in the Princeton Ocean Model (POM) and applied to the Labrador Sea and the Grand Banks to simulate surface currents. A wave model, WAVEWATCH III, is used to calculate the Stokes drift and momentum transfers among winds, waves and currents. Four surface drifters deployed on the Grand Banks in October 2002 provide a test data set.

## 2. Current-wave and current-drifter coupling

The computation of surface currents involves both the wave and ocean dynamics. The governing equations for surface currents are a set of Navier-Stokes equations modified by waves. The wave spectrum and the solution of the modified Navier-Stokes equations are obtained from a wave model and a 3-d circulation model described in Section 3. To compare the model surface currents with velocities derived from surface drifters, knowledge of the response of the drifters to air drag is required. A simple model of surface drifter is developed in Section 2.2 to calculate the correction of drifter velocities due to the air drag.

### 2.1 Current-wave coupling

Ocean currents with time scales of variability much longer than the wave periods can be written as the sum of three terms:

$$\mathbf{U} = \mathbf{u}_s + \mathbf{u}_t + \mathbf{u} \tag{1}$$

where $\mathbf{u}_s$ is the Stokes drift, $\mathbf{u}_t$ is the tidal current and $\mathbf{u}$ is the Eulerian mean current. $\mathbf{u}_s$ can be computed from 2-dimensional wave energy spectrum, $E(f,\theta)$, by

$$\mathbf{u_s} = 4\pi \iint f\mathbf{k} e^{2kz} E(f,\theta) df d\theta \tag{2}$$

where $f$ is wave frequency and $\theta$ is wave direction. The wave spectrum, $E(f,\theta)$, is governed by the wave energy equation:

$$\frac{\partial E(f,\theta)}{\partial t} + \mathbf{C_g} \cdot \nabla E(f,\theta) = S_{in} + S_{ds} + S_{nl} \tag{3}$$

where $\mathbf{C_g}$ is the group velocity of waves. $S_{in}$,, $S_{ds}$ and $S_{nl}$ are the source terms for wave generation, dissipation and non-linear energy transfer, respectively.

The tidal current, $\mathbf{u}_t$, was calculated from a barotropic tidal model for the eastern Canadian shelves (Han et al., 1996). The model includes major semidiurnal ($M_2$, $S_2$, $N_2$) and diurnal ($K_1$, $O_1$) tides.

The Eulerian mean current, $\mathbf{u}$, is governed by a set of modified Navier-Stokes equations. The momentum equation has the following form:

$$\frac{d\mathbf{u}}{dt} + \mathbf{f} \times (\mathbf{u} + \mathbf{u_s}) = -\frac{1}{\rho_o} \nabla p + \frac{\partial}{\partial z}\left(K_m \frac{\partial \mathbf{u}}{\partial z}\right) + \mathbf{F}_{ds} \tag{4}$$

where $\mathbf{u}$ is also denoted as the quasi-Eulerian current since it also refers to the Lagrangian mean fluid particle positions. In (4), $\mathbf{f}$ is the Coriolis parameter, $p$ is pressure, $K_m$ is the vertical eddy viscosity, and $\mathbf{F}_{ds}$ is the wave-induced momentum transfer from waves to ocean due to dissipation of wave energy, which we assume is distributed in the vertical in the same way as the Stokes drift:

$$\mathbf{F}_{ds} = -4\pi \iint f\hat{\mathbf{k}} S_{ds} k e^{2kz} df d\theta \qquad (5)$$

where $\hat{\mathbf{k}}$ is a unit vector in the direction of **k**.

The boundary condition at the sea surface is:

$$K_m \frac{\partial \mathbf{u}}{\partial z}\Big|_{z=0} = \frac{1}{\rho_o}(\mathbf{T}_a - \mathbf{T}_{in}) \qquad (6)$$

where $\mathbf{T}_a$ is the wind stress and $\mathbf{T}_{in}$ is the reduction of wind stress due to wave generation. Jenkins (1989) proposed the following form for $\mathbf{T}_{in}$:

$$\mathbf{T}_{in} = 2\pi\rho_o \iint f\hat{\mathbf{k}} S_{in} df d\theta \qquad (7)$$

Close to the sea bottom, the velocity profile follows the law of the wall and the bottom stress is assumed a quadratic function of water velocity with a drag coefficient determined from the apparent bottom roughness.

### 2.2 Current-drifter coupling

The velocity data used in this study are derived from the trajectories of surface drifters. The drifter velocity deviates from the velocity of surface water because wind stress acting on the exposed part of the drifter exerts a force on the drifter that drives it downwind with respect to the surface water in which it resides. The difference between the drifter and surface water velocity, known as leeway, may be estimated from a simple dynamical model of surface drifter.

The governing equation for the velocity of a surface drifter, $\mathbf{U}_b$, can be written as:

$$m\left(\frac{d\mathbf{U}_b}{dt} + \mathbf{f} \times \mathbf{U}_b\right) = -mg\nabla\varsigma + \mathbf{F}_{air} - \mathbf{F}_{water} \qquad (8)$$

where $m$ is the mass of the drifter. $\mathbf{F}_{air}$ and $\mathbf{F}_{water}$ are the drag forces on above- and below-surface portions of the drifter, respectively. They can be parameterized by quadratic equations:

$$\mathbf{F}_{air} = \frac{1}{2}\rho_a C_{da} A_a |\mathbf{W}|\mathbf{W} \qquad (9)$$

$$\mathbf{F}_{water} = \frac{1}{2}\rho_o C_{dw} A_w |\mathbf{U}_b - \mathbf{U}(0)|[\mathbf{U}_b - \mathbf{U}(0)] \qquad (10)$$

where **W** is 10-m wind, $C_{da}$ and $C_{dw}$ are the air and water drag coefficients, and $A_a$ and $A_w$ are the exposed cross sectional areas of the drifter above and below the water surface, respectively. They can be estimated from empirical data. **U**(0) is surface velocity defined by (1). In (10), we have assumed that ocean currents do not have a large vertical variation over the submerged portion (draft) of the drifter.

$\mathbf{U}_b$ can be solved numerically given **U**(0), **W** and sea surface elevation. If the dominant timescales of the wind greatly exceed the dynamic response time of the drifter and the leeway component of the drift current is small ($\mathbf{f} \times \mathbf{U_b} \approx \mathbf{f} \times \mathbf{U}(0) \approx mg\nabla\zeta$), the drag forces on the drifter are approximately in equilibrium ($\mathbf{F}_{air} \approx \mathbf{F}_{water}$), so that:

$$|\mathbf{U}_b - \mathbf{U}(0)|[\mathbf{U}_b - \mathbf{U}(0)] = r^2 |\mathbf{W}|\mathbf{W} \qquad (11)$$

where $r^2 = (\rho_a C_{da} A_a / \rho_w C_{dw} A_w)$ is a ratio of drag parameters. $\mathbf{U}_b$ can be solved algebraically from (11) given **U**(0) and **W**.

### 3. Ocean model and wave model

The ocean model used in this work is a modification of the Princeton Ocean Model (POM) implemented for the eastern Canadian seas by Yao et al. (2000). The model domain (Fig. 1) is from 40° N to 66° N and from 40° W to 58° W. The vertical levels have been increased from 16 in Yao et al. (2000) to 23 ( $z$/D= 0, 0.0004, 0.0012, 0.0028, 0.006, 0.012, …..).

The vertical eddy viscosity is a function of time, depth and position. It has the form:

$$K_m = lqS_m \qquad (12)$$

The vertical profiles of $l$, the mixing length, and $q^2/2$, the turbulence kinetic energy, are determined by solving the equations for $q^2$ and $q^2 l$ in a turbulence closure model embedded in POM. The stability function $S_m$ depends on vertical shear, buoyancy, $q$ and $l$.

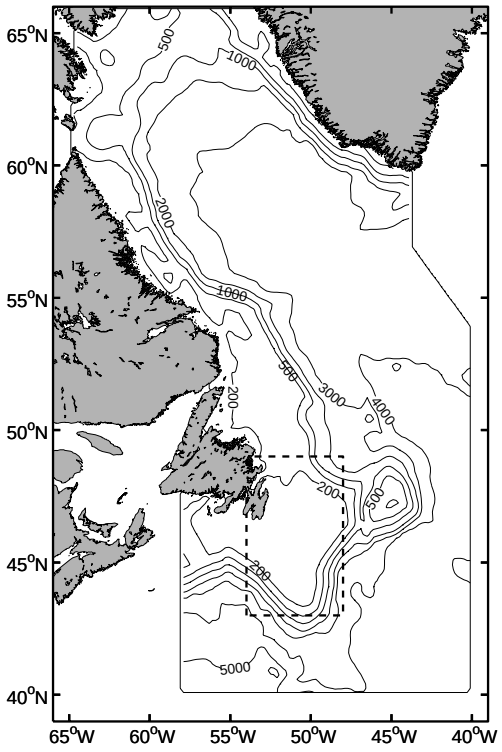


Fig. 1. POM model domain and bathymetry. The rectangle indicates the study area.

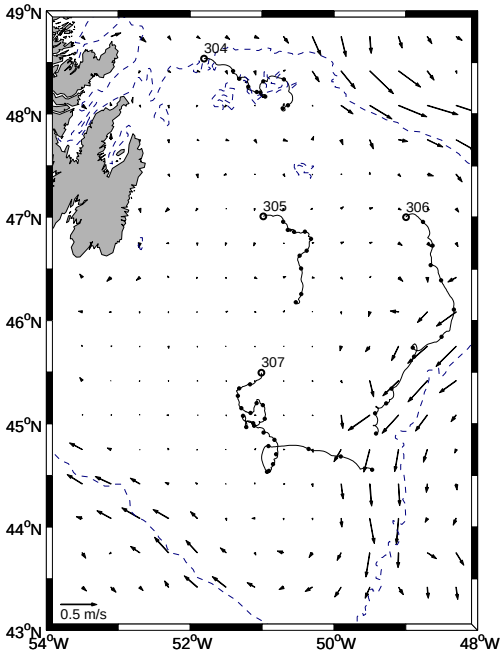


Fig. 2. Model mean currents (arrows) and drifter trajectories on the Grand Banks. The dots on the trajectories indicate one-day intervals. The numbers are drifter identification (Table 1). The open circles indicate the start points of the trajectories. The dash line is 2000 m isobath.

The surface velocities from a spin-up run of the model (without the tidal currents) representing the mean surface currents are shown in Fig. 2. The most prominent feature of the mean current field is the strong Labrador Current along the eastern shelf edge of the Grand Banks. Currents in the interior of the Grand Banks are relatively weak.

The wave model used in this study is WAVEWATCH III (hereafter WW3), version 2.22. It is a discrete spectral phase-averaged model (Tolman, 2002), which resolves the directional spectrum at each model grid point in terms of wavenumber-direction bands.

Two formulations for $S_{in}$,, $S_{ds}$ are considered in this study: the conventional cycle3 WAM formulations for $S_{in}$ and $S_{ds}$ of the WAMDI Group (1988), as the base experiment (Section 5), and the more recent $S_{in}$,, $S_{ds}$ default "wave-boundary layer" parameterizations of Tolman and Chalikov (1996) in WW3 (hereafter denoted the 'WW3' formulation) in the sensitivity experiment (Section 6).

## 4. Wind and surface drifter data

The forcing for the model is 6-hourly 10-m winds on a $1^{o}$x$1^{o}$ grid from Meteorological Service of Canada. Surface heat and mass fluxes are set to zero.

Four surface drifters were deployed on the Grand Banks in October 2002 by Canadian Coast Guard (Fig. 2, Table 1). The duration varies from 11 to 23 days. The drifters, SLDMB (Self-Locating Datum Marker Buoy manufactured by Seimac Ltd.), were designed to track the surface water with minimal leeway.

**Table 1.** Information on drifter data.

| Drifter ID | Start | Duration (day) |
|---|---|---|
| 304 | 1200 October 8 | 11 |
| 305 | 1200 October 8 | 11 |
| 306 | 1200 October 8 | 13 |
| 307 | 1200 October 9 | 23 |

## 5. Comparison of model simulations with data

The effects of waves on surface currents are investigated from three base model experiments:

(a) No waves. The quantities $\mathbf{u}_s$ , $F_{ds}$ and $T_{in}$ in (1), (4) and (6) are set to zero;

(b) Full wave effects. The velocity **u** is computed from the full equations, plus the Stokes drift and the tidal currents;

(c) Stokes drift only and no air-wave-momentum transfer. Set $F_{ds}$ and $T_{in}$ to zero but keep the Coriolis term associated with the Stokes drift in (4) and add the Stokes drift and the tidal currents.

A standard set of parameter values within their allowable ranges is adopted (Table 2) in order to generate reasonable simulations of the observed drift trajectories. In Table 2, $\beta$ is a parameter of $l$, $z_{oa}$ is the apparent bottom roughness resulting from wave-current interactions (Grant and Madsen, 1979). The effects of waves on the drift can be deduced from the analysis of the results of the three experiments.

The model currents were averaged over the top 1 m in order to avoid bias associated with the variable vertical grid size.

**Table 2.** Parameter values in the base experiments.

| **Model** | **Sym-bol** | **Value in base runs** | ***Parameters*** |
|---|---|---|---|
| Ocean model | $\beta$ | $4 \times 10^{-5}$ | Mixing length parameter |
| | $z_{oa}$ | 0.1 m | Apparent bottom roughness |
| Drifter model | $r^2$ | $0.18 \times 10^{-4}$ | Drag parameter ratio |
| Wave model | WAM | $S_{in}$ and $S_{ds}$ parameterizations from WAMDI Group | |

### 5.1 Overall comparison of the trajectories

Fig. 3 shows the observed (black) and modelled trajectories with (blue and green) and without (red) the wave effects. The modelled and observed trajectories diverge with time as expected. Overall, the trajectories without the wave effects are too short and tend to veer to the right of the drifter trajectories. The difference between Experiments (b) (blue) and (c) (green) is not large.

The errors shown in Fig. 3 are cumulative errors starting from four given initial positions. A better measure of the errors can be obtained from trajectory segments initialized at different starting times and locations along the drifter trajectories. This is carried out in the following sub-section.

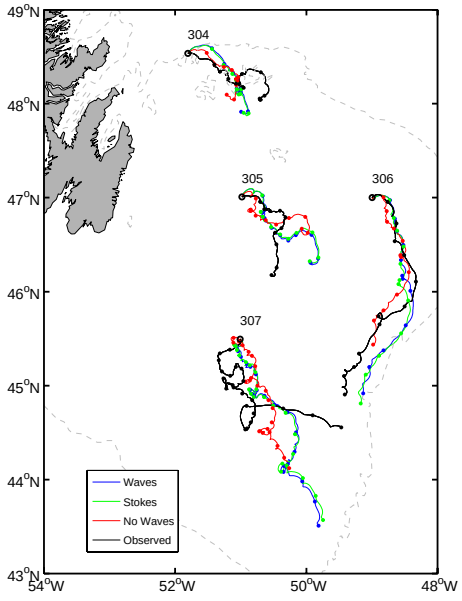


Fig. 3. Surface drifter trajectories from the observation (black) and three model experiments: (a) red (no wave); (b) blue (full wave effects); (c) green (Stokes drift only).

### 5.2 Separation as a function of time

The drifter trajectories were broken up into segments of varying time intervals. For each segment, the separation between the end points of the modelled and observed trajectories were calculated. By including the wave effects, the mean separation decreases from 12 km to 9.5 km at day 1, and from 20.5 km to 17 km at day 2 (left panel of Fig. 4). These figures represent an improvement of 21 % at day 1 and 17 % at day 2 from the model run without waves to that with the wave effects. The difference between Experiments (b) and (c) is relatively small with the Stokes drifts only experiment (dashed line) showing a slightly smaller separation. This difference may not be statistically insignificant because of the small number of drifters.

To remove the influence of mean current in the statistics, separations normalized by the length of the observed trajectories were computed (right panel of Fig. 4). The relative errors decrease with time. A possible explanation for the decreasing relative errors is that short-period motions such as inertial oscillation and diffusion are not well simulated by the model. With the

selected model parameters (Table 2), the model with the wave effects can achieve a relative error of 0.52 at day 1 and 0.43 at day 2.

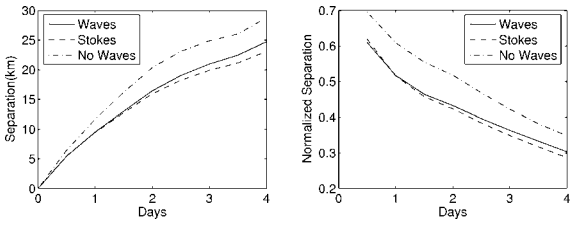


Fig. 4. Mean separation (left) and normalized separation (right) as a function of time from the three model experiments: (a) dash-dotted lines (no wave); (b) solid lines (full wave effects); (c) dash lines (Stokes drift only).

### 5.3 Vector regression analysis

To assess the wave effects on surface velocity quantitatively, a vector regression analysis was carried out. The drifter velocity is assumed to be the sum of a wind-driven component and a non-wind- driven component. The former is taken to be wind velocity reduced by a factor $R$ and rotated by an angle $\phi$. In complex notation, the relation between the drifter velocity, $U_b$, and the wind, $W$, can be written as:

$$U_b = R \cdot W \exp(i\phi) + U_0 \qquad (13)$$

where $U_o$ is the velocity of non-wind driven motion. A negative $\phi$ means the drifter direction is rotated clockwise from the wind direction. We shall call $R$ the speed ratio and $-\phi$ the turning angle. Given time series $U_b$ and $W$, (13) can be used to determine the best values for $R$, $\theta$ and $U_0$ from a least square fit.

The vector regression analysis was carried out for each drifter and the three base experiments separately. For each assembly of vector pairs, a correlation coefficient can be obtained. We follow the method of Crosby et al. (1993) to compute the correlation coefficients between two vector time series. The range of the coefficient is from 0 to 2. The correlation coefficients for #306 are low (0.44 for the model and 0.47 for the data). This implies that the relationship between wind and surface current is not a linear one. Factors other than wind, such as pressure gradient and shelf wave can be more important in driving the current. A large portion of the trajectory of Drifter 306 is in the Labrador Current (Fig. 2) where pressure gradients are enhanced and shelf waves generated upstream propagating to the Grand Banks have a maximum magnitude (Tang et al., 1998). Both the pressure gradients and shelf waves can be generated by wind but they are not directly correlated to the wind vectors as opposed to the Ekman currents in an ocean without lateral boundary.

The correlation coefficients for the three drifters on the Grand Banks (304, 305, 307) range from 0.61 to 1.27. The results of the regression analysis shown in Table 3 are the averages of the three drifters weighted by the correlation coefficients. On average, the observed drifter speeds are 2.06% of the wind speeds and the directions are 30° clockwise from the wind directions. The model with wave-current coupling, Experiment (b), gives reasonably good simulations with a mean speed ratio of 2.07% and a mean turning angle of 34°. The increase of surface speed from Experiments (a) to (b) is 35%. The simulation without the wave effects, Experiment (a), under-predicts the speed ratio by 0.52% and over-predict the turning angle by 28°.

**Table 3.** Speed ratio (SR), turning angle (TA) and correlation coefficient (CC) between winds and surface velocities for the three drifters on the Grand Banks (304, 305, 307, 307) from the vector regression analyses of the data and the model: (a) no wave; (b) full wave effects; (c) Stoke drift only. The range of correlation coefficient is 0 to 2.

| | **Obs.** | **Model** | | |
|---|---|---|---|---|
| | | **(a)** | **(b)** | **(c)** |
| **SR (%)** | 2.06 | 1.54 | 2.07 | 2.08 |
| **TA (deg)** | 30.2 | 58.0 | 33.9 | 35.3 |
| **CC** | 0.97 | 0.71 | 0.99 | 0.95 |

The relative contributions of the Stokes drift and momentum transfer to the surface velocities can be estimated by comparing Experiments (b) and (c) in Table 3. The Stokes drift increases the speed ratio by 0.54% (from (a) to (c)). The air-wave-current momentum transfers decrease the surface currents slightly (from (c) to (b)) but the difference between them is not significant. The change in the drifter direction from 58° (no wave) to 34° (with waves) is largely due to the Stokes drift.

The moderate correlation coefficient for the observed drifter velocity indicates that a sizable portion of the surface currents is not directly correlated to winds. This may include tidal current, meso-scale eddies and random diffusion. The correlation coefficient from the model run with the wave effects, (b), has a comparable magnitude, and is significantly larger than the correlation coefficients from (a).

## 6. Sensitivity experiments and errors

The wave and drifter models have several adjustable parameters including $\beta$ in the eddy viscosity, apparent bottom roughness $z_{ao}$, drag parameter ratio $r$ and the $S_{in}$ and $S_{ds}$ terms in the wave spectrum. To assess the sensitivity of the model to these parameters, we conducted six additional model experiments (Table 4) each with one parameter value different from the base experiments (Table 2). The results indicate that in general the changes in the parameter values have minimal effect on the turning angle, and the range of the speed ratio in Table 4 is much smaller than the difference between Experiments (a) and (b) in the base experiments (Table 3).

**Table 4.** Comparison of speed ratio (SR), turning angle (TA) (clockwise from the wind direction in degree) and correlation coefficient (CC) between the base and sensitivity experiments. The values shown are the means of Drifter 304, 305 and 307 weighted by the correlation coefficients. The range of correlation coefficient is 0 to 2.

| Para-meter | Value | SR (%) | TA (deg) | CC |
|---|---|---|---|---|
| Base set | Table 2 | 2.07 | 33.9 | 0.99 |
| $\beta$ | $2 \times 10^{-5}$ | 2.32 | 33.6 | 1.10 |
| $z_{oa}$ | 0.5 m | 2.06 | 33.7 | 1.00 |
| $r^2$ | $0.4 \times 10^{-4}$ | 2.13 | 32.3 | 1.00 |
| $S_{in}$,, $S_{ds}$ | WW3 | 1.99 | 35.9 | 0.94 |

$\beta$ control the mixing length and hence the profile of the eddy viscosity, $K_m$ , near the surface. A decrease of $\beta$ by 50% results in an increase of surface current by 12%. The increase is closely related to the profile of eddy viscosity near the surface. Fig. 5 shows the mean eddy viscosity for $\beta = 4 \times 10^{-5}$ and $2 \times 10^{-5}$ at low (left panel) and high wind speeds (right panel) computed from a 1-d version of POM. At low wind speeds, the profiles below 3 m have the conventional form of a maximum in the mixed layer. At high wind speeds, $K_m$ decreases monotonically with depth.

In the presence of waves, the apparent bottom roughness, $z_{ao}$ , is a function of wave orbital velocity and friction velocity near the bottom. Its value can be one or more orders of magnitude larger than the actual roughness (Grant and Madsen, 1979; Mellor 2002). For the Grand Banks, the apparent bottom roughness is estimated to be 5 to 100 times of the actual roughness. Table 4 shows that changing $z_{ao}$ from 0.1 m to 0.5 m decreases the surface current slightly.

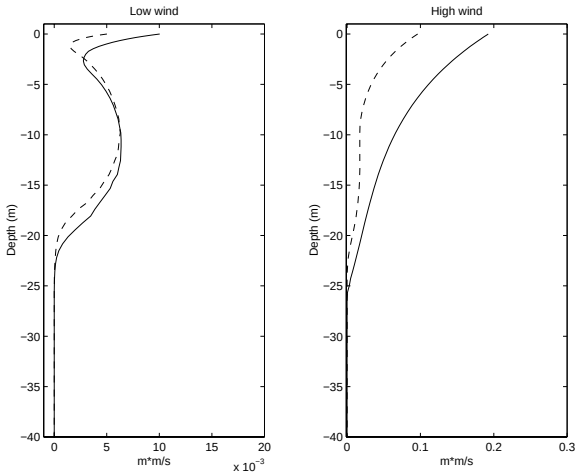


Fig. 5. Mean eddy viscosity profiles from the 1-d version of POM. Left panel is for wind speeds less than 5 $ms^{-1}$. Right panel is for wind speeds greater than 10 $ms^{-1}$. The solid lines are for $\beta = 4 \times 10^{-5}$ in the base experiments. The dash lines are for $\beta = 2 \times 10^{-5}$ in the sensitivity experiment.

The estimated value of $r^2$ in the base run (Table 2) is based on the frontal areas (in air and water) of the SLDMB and its two drogues. An increasing of $r^2$ from $0.18 \times 10^{-4}$ to $0.4 \times 10^{-4}$ leads to an increase of the speed ratio by 0.06% (Table 4). The small increase from the model simulation is due to the fact that only the downwind component of surface velocity will be enhanced by leeway.

The wind input $S_{in}$ and dissipation $S_{ds}$ parameterizations used in Table 4 are the formulations of Tolman and Chalikov (1996) (denoted WW3). These $S_{in}$,, $S_{ds}$ parameterizations result in a reduction in surface speed by about 4%, relative to the base experiment using the older WAM cycle3 parameterizations and a slight modification in the turning angle. This result is consistent with the tendency for the former to give slight overall reductions in wave growth, compared to earlier WAM cycle3 formulations.

## 7. Summary and concluding remarks

There are two major wave effects in Jenkins' theory, the Stokes drift and air-wave-current momentum transfers. The Stokes drift can increase surface current speed significantly, by 35%, and turn the currents toward the wind direction. The momentum transfers can reduce the surface speed slightly and have minimal effect on the directions. On average, the observed drifter speeds are 2.06% (speed ratio) of wind speeds and the directions are 30° clockwise from wind direction. Without wave-current coupling, the model

under-predicts the speed ratio by 0.52% and over-predicts the turning angle by 28°. The model performance can also be measured by the separation between the modelled and drifter trajectories. The improvement from the model without waves to the model with waves is approximately 21% at day 1 and 17% at day 2.

There are uncertainties in the model parameters. The speed ratio is most sensitive to the surface eddy coefficient, moderately sensitive to wave spectrum and air drag and least sensitive to bottom friction. The turning angle is not sensitive to any parameter.

There are other sources of uncertainty such as errors in wind data and the relationship between surface wind and stress. In particular, small-scale winds may be absent from the wind data we used, which could contribute to further errors in the modelled surface currents. Such errors are unrelated to wave-ocean interactions.

***Acknowledgments***

The research has been supported by the Canadian Panel on Energy Research & Development, the Canadian Coast Guard NIF, the Canada Foundation for Atmospheric and Climate Studies CFCAS, and SURA, the Southeast University Research Association through SCOOP, the SURA Coastal Ocean Observing Program. We thank A. D. Jenkins, B.M. Detracey, Y.Hu and B. Toulany for their contribution to the work. J. Maillette, K. MacIntyre and R. Dawson of the Canadian Coast Guard deployed the surface drifters used in this study and made the data available to us.

**References**

Crosby, D.S., L.C. Breaker and W.H. Gemmill, 1993: A proposed definition for vector correlation in Geophysics: theory and application. J. Phys. Oceanogr., **10**, 355-367.

Grant, W.D. and O.S. Madsen, 1979: Combined wave and current interaction with a rough bottom. J. Geophys. Res., 84, 1797-1808.

Han, G., M. Ikeda and P.C. Smith, 1996: Oceanic tides over the Newfoundland and Scotian Shelves from TOPEX/POSEIDON altimetry. Atmosphere-Ocean, **34**, 589-604.

Jenkins, A.D., 1987: Wind and Wave Induced Currents in a Rotating Sea with Depth-Varying Eddy Viscosity. J. Phys. Oceanogr., **17**, 938-951.

Jenkins, A.D., 1989: The use of a wave prediction model for driving a near-surface current model. Dt. Hydrog. Z., **42**, 133-149.

Mellor, G., 2002: Oscillatory bottom boundary layers. J. Phys. Oceanogr., **32**, 3075-3088.

Perrie, W., C.L. Tang, Y. Hu and B.M. DeTracey, 2003: The impact of waves on surface currents. J. Phys. Oceanogr., **33**, 2126-2140.

Tang, C.L., Q. Gui and B.M. DeTracey, 1998: Barotropic response of the Labrador/Newfoundland shelf to a moving storm. J. Phys. Oceanogr., **28**, 1152-1191.

Tolman, H.L. and D. V. Chalikov, 1996: Source terms in a third-generation wind wave model. J. Phys. Oceanogr., 26, 2497-2518.

Tolman, H.L., 2002: User manual and system documentation of WAVEWATCH-III version 2.22. Technical Note. [Available online at http://polar.ncep.noaa.gov/waves].

WAMDI Group, 1988: The WAM model – a third generation ocean wave prediction model. *J. Phys. Oceanogr.*, **18**, 1775-1810.

Yao, T., C.L. Tang and I.K. Peterson, 2000: Modeling the seasonal variation of sea ice in the Labrador Sea with a coupled multi-category ice model and the Princeton Ocean Model. J. Geophys. Res., **105**, 1153-1165.